AD-A039 174 NAVAL AIR TEST CENTER PATUXENT RIVER MD F/G 1/1
THE DEVELOPMENT OF PRIMARY EQUATIONS FOR THE USE OF ON-BOARD AC--ETC(U)
APR 77 W R SIMPSON

UNCLASSIFIED NATC-TM-76-3-SA NL

1 OF 1
AD A039174

END

DATE FILMED
5 - 77

AD A039174

FG.

12

TM 76-3 SA

Technical Memorandum

THE DEVELOPMENT OF PRIMARY EQUATIONS FOR THE USE OF ON-BOARD ACCELEROMETERS IN DETERMINING AIRCRAFT PERFORMANCE

W. R. Simpson
Strike Aircraft Test Directorate

DDC
RECEIVED
MAY 10 1977
C

19 April 1977

DDC FILE COPY

Approved for public release;
distribution unlimited.

NAVAL AIR TEST CENTER
PATUXENT RIVER, MARYLAND

UNCLASSIFIED

SECURITY CLASSIFICATION OF THIS PAGE (When Data Entered)

REPORT DOCUMENTATION PAGE

READ INSTRUCTIONS BEFORE COMPLETING FORM

1. REPORT NUMBER: TM 76-3 SA
2. GOVT ACCESSION NO.:
3. RECIPIENT'S CATALOG NUMBER:

4. TITLE (and Subtitle): THE DEVELOPMENT OF PRIMARY EQUATIONS FOR THE USE OF ON-BOARD ACCELEROMETERS IN DETERMINING AIRCRAFT PERFORMANCE.

5. TYPE OF REPORT & PERIOD COVERED: TECHNICAL MEMORANDUM

6. PERFORMING ORG. REPORT NUMBER:

7. AUTHOR(s): W. R. SIMPSON

8. CONTRACT OR GRANT NUMBER(s):

9. PERFORMING ORGANIZATION NAME AND ADDRESS:
NAVAL AIR TEST CENTER
NAVAL AIR STATION
PATUXENT RIVER, MARYLAND 20670

10. PROGRAM ELEMENT, PROJECT, TASK AREA & WORK UNIT NUMBERS:

11. CONTROLLING OFFICE NAME AND ADDRESS: NATC-TM-76-3-SA

12. REPORT DATE: 19 APRIL 1977

13. NUMBER OF PAGES: 28

14. MONITORING AGENCY NAME & ADDRESS (if different from Controlling Office): 27p.

15. SECURITY CLASS. (of this report): UNCLASSIFIED

15a. DECLASSIFICATION/DOWNGRADING SCHEDULE:

16. DISTRIBUTION STATEMENT (of this Report)

APPROVED FOR PUBLIC RELEASE; DISTRIBUTION UNLIMITED.

17. DISTRIBUTION STATEMENT (of the abstract entered in Block 20, if different from Report)

DDC PROCESSED MAY 10 1977 C

18. SUPPLEMENTARY NOTES

19. KEY WORDS (Continue on reverse side if necessary and identify by block number)

ACCELEROMETERS
AIRCRAFT PERFORMANCE
DYNAMIC PERFORMANCE
FLIGHT TEST

20. ABSTRACT (Continue on reverse side if necessary and identify by block number)

Primary equations for the use of on-board accelerometer data (both flight path and body mounted) for determining aircraft performance are developed. Primary equations are those mathematical relationships which relate measured quantities to useful parameters. They are distinguished from secondary and analysis equations in that the latter are used to either standardize or separate effects in the data. Reference materials are cited, or methods are presented for obtaining all parameters necessary in the use of the primary → next page

DD FORM 1 JAN 73 1473 EDITION OF 1 NOV 65 IS OBSOLETE

UNCLASSIFIED

SECURITY CLASSIFICATION OF THIS PAGE (When Data Entered)

20.

cont →

equations. In cases where sufficient reference materials are not available, the equations are derived. An equation summary is presented for the user who does not wish to go through the development procedures.

PREFACE

Primary equations for the use of on-board accelerometer data (both flight path and body mounted) for determining aircraft performance are developed. Primary equations are those mathematical relationships which relate measured quantities to useful parameters. They are distinguished from secondary and analysis equations in that the latter are used to either standardize or separate effects in the data. Reference materials are cited, or methods are presented for obtaining all parameters necessary in the use of the primary equations. In cases where sufficient reference materials are not available, the equations are derived. An equation summary is presented for the user who does not wish to go through the development procedures.

APPROVED FOR RELEASE

RADM J. H. FOXGROVER, USN
COMMANDER, NAVAL AIR TEST CENTER

TABLE OF CONTENTS

LIST OF ILLUSTRATIONS

INTRODUCTION

1. The determination of aircraft performance has become increasingly complex in recent years. This is not only because the aircraft systems themselves have become more complex with time making their investigation more difficult, but principally because of a general shift in philosophy of aircraft performance analysis from the direct method to the indirect method. This shift has come about because of the generally larger volume of data available in less flight time by the indirect method.

2. The direct method is characterized by flying a particular maneuver of interest and mathematically correcting this maneuver to a given set of standard conditions. Several similar maneuvers at different flight conditions are then combined in a composite map representing one aspect of the aircraft's performance. For example, families of stabilized points at different constant values of W/δ are used to represent aircraft specific range; or specific excess power is calculated from several accelerations at different altitudes and combined to represent the ability of the aircraft to change its energy state.

3. The indirect method is more subtle and has its basis deeper in theory. By this method, a group of aerodynamic and propulsion parameters are developed from flight tests. The parameters in themselves are only numbers and do not represent performance. These parameters are not tied to a specific maneuver or maneuver type but, in general, relate the physical forces required to achieve a certain flight condition. Such parameters for an aircraft would be the drag coefficient, lift coefficient, referred thrust, referred fuel flow, etc. However, these parameters can be combined with known aircraft characteristics to derive the airplane performance. For example, the airplane drag polar and thrust-fuel flow requirements can be coupled to develop aircraft specific range data.

4. The relation of measured quantities to some desired information about a system has been a problem facing the experimentalist since the first experiments were performed. The problem arises from the inability to measure directly a desired quantity in all instances. Many measurements by parametrics are taken as a matter of course. For example, engine pressures and temperatures are measured to infer engine thrust output. Other parametric measurements are more subtle, such as the measurements of airspeed and altitude, which are, in reality, parametrically measured by pressures and mechanically converted to the desired parameters in the output instrument.

5. With on-board accelerometers, then the question arises: given the measurement of aircraft acceleration, how does one arrive at aircraft performance parameters? In order to answer this question, the aircraft force balance system must be examined. Additionally, the measurement of acceleration must be examined to determine its relation to the aircraft system. Finally, examination must be made of factors which affect either the aircraft force balance system or the measurement of accelerations.

DEVELOPMENT OF EQUATIONS

AIRCRAFT FORCE BALANCE

6. The various forces contributing to a change in specific energy (E_s) of an aircraft can be found by analyzing figure 1. The E_s is a measure of the total kinetic and potential energy of an aircraft. For ease of calculation, forces will be resolved parallel and perpendicular to the direction of flight (wind axis system). In the general case, the aircraft may be taken to be both climbing and accelerating. The simplified model developed herein assumes wings level flight at zero sideslip for the purpose of clarity. The effects of bank angle and sideslip will be discussed later. Additionally, the gross thrust vector is assumed to lie in the x-z plane. Toe-out effects can be accounted for by simply viewing the gross thrust vector as the in-plane component.

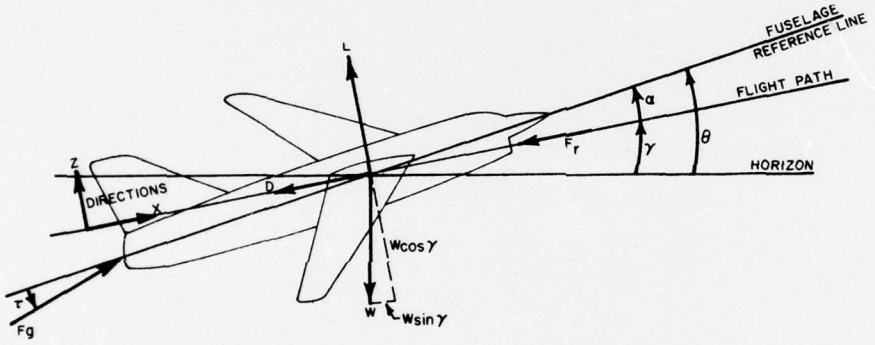

Figure 1
Aircraft Force Balance Diagram

7. Resolving forces along the flight path and assuming the mass change to be instantaneously zero:

$$\Sigma F_x = ma_x \tag{1}$$

$$F_g \cos(\alpha+\tau) - F_r - D - W\sin\gamma = \frac{W}{g} ax_{A/C} = \frac{\dot{W}}{g}\frac{dVt}{dt} \tag{2}$$

defining the net thrust (F_n) as:

$$F_n = F_g \cos(\alpha+\tau) - F_r \tag{3}$$

equation (2) can be rewritten as:

$$F_n - D - W\sin\gamma = \frac{W}{g}\frac{dVt}{dt} \tag{4}$$

or

$$F_{ex} \triangleq F_n - D = W\left(\frac{1}{g}\frac{dVt}{dt} + \sin\gamma\right) \tag{5}$$

8. The ram drag (F_r) is assumed to act along the flight path and can be obtained from on-board inlet instrumentation or engine manufacturer's curves of airflow (W_a) and by the equation:

$$F_r = W_a V_t \tag{6}$$

9. For forces perpendicular to the flight path, the equation becomes:

$$\Sigma F_z = ma_z \tag{7}$$

$$L - W\cos\gamma + F_g \sin(\alpha+\tau) = \frac{W}{g} a_{z_{A/C}} \tag{8}$$

or:

$$L = W\left(\cos\gamma + \frac{a_{z_{A/C}}}{g}\right) - F_g \sin(\alpha+\tau) \tag{9}$$

Equations (5) and (9) become the force balance equations of the aircraft in the two dimensional wind axis system (assuming zero sideslip and wings level).

10. Having resolved the force balance equations for the aircraft and defined excess thrust and lift as functions of accelerations, the next step is to select an accelerometer package for measuring these accelerations. The accelerometer package can be either mounted in the boom and mechanically connected to the angle of attack vanes where it is free to align itself with the flight path of the aircraft, or it can be hard mounted in the body of the aircraft. Each case will be examined separately.

FLIGHT PATH ACCELEROMETER PACKAGE

11. The angular relations of the flight path accelerometer can be resolved through the use of figure 2. For clarification, angle of attack system misalignment, boom bending, and dynamic errors in angle of attack have been eliminated from the figure.

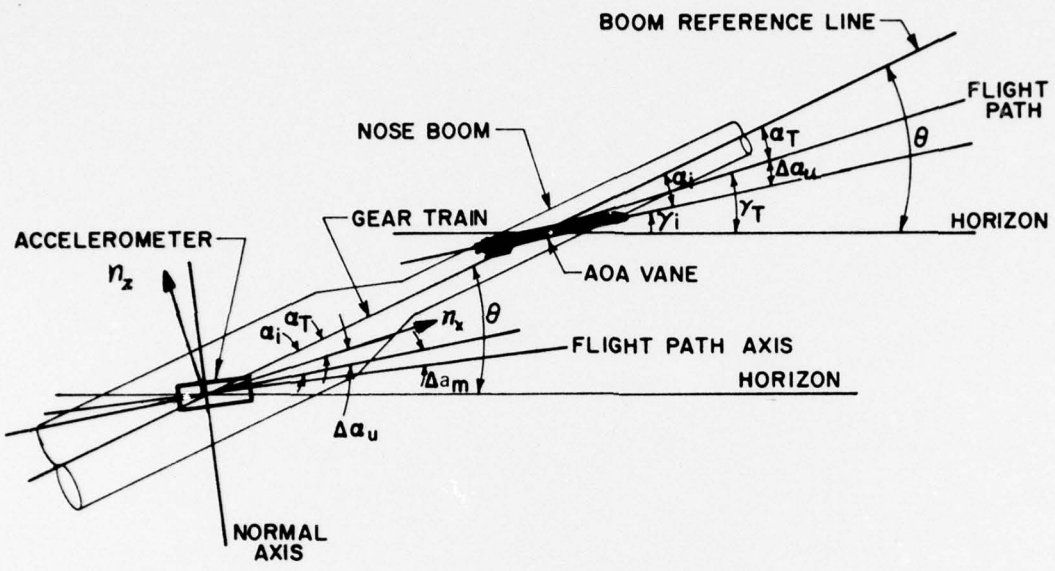

Figure 2
Flight Path Accelerometer Balance Diagram

The α_t referred to here is the true angle of attack of the boom reference line, and under 1 g conditions, this will be the true angle of attack since the upwash calibration will include the aerodynamic boom bending. In the general case of accelerated flight, the boom bending term ($\Delta\alpha_{BB}$) should be added at this point so that:

$$\alpha_t = \alpha_i + \Delta\alpha_{upwash} + \Delta\alpha_{BB} \tag{10}$$

where $\Delta\alpha_{BB}$ is a function of normal acceleration at the boom and pitch acceleration ($\ddot{\theta}$) and is determined from laboratory calibrations as discussed in reference (a). Further effects of angular rates and their derivatives are given in paragraphs 27 to 30. The accelerometer is aligned with the angle of attack vane with the exception of a misalignment angle due to mechanical fitting (Δa_m). The determination of these misalignments which may, in general, be different for the normal and flight path axes is discussed in detail in reference (a). The accelerometer flight path axis is then misaligned from the flight path by:

$$\Delta\alpha_{total} = \Delta\alpha_{upwash} + \Delta a_m + \Delta\alpha_{BB} \tag{11}$$

12. Resolving the readings of the accelerometer to the proper axes (along and perpendicular to the flight path):

$$a_{x_{FPA}} = a_{xi_{FPA}} \cos(\Delta\alpha_u + \Delta a_{m_{x_{FPA}}} + \Delta\alpha_{BB}) - a_{z_{i_{FPA}}} \sin(\Delta\alpha_u + \Delta a_{m_{z_{FPA}}} + \Delta\alpha_{BB}) \quad (12)$$

$$a_{z_{FPA}} = a_{xi_{FPA}} \sin(\Delta\alpha_u + \Delta a_{m_{x_{FPA}}} + \Delta\alpha_{BB}) + a_{z_{i_{FPA}}} \cos(\Delta\alpha_u + \Delta a_{m_{z_{FPA}}} + \Delta\alpha_{BB}) \quad (13)$$

It is often more convenient to work with the accelerations in g units or measurements of load factors, and the accelerometers will be calibrated in terms of load factor such that the above equations become:

$$n_{x_{FPA}} = n_{xi_{FPA}} \cos(\Delta\alpha_u + \Delta a_{m_{x_{FPA}}} + \Delta\alpha_{BB}) + n_{zi_{FPA}} \sin(\Delta\alpha_u + \Delta a_{m_{z_{FPA}}} + \Delta\alpha_{BB}) \quad (14)$$

$$n_{z_{FPA}} = n_{xi_{FPA}} \sin(\Delta\alpha_u + \Delta a_{m_{x_{FPA}}} + \Delta\alpha_{BB}) + n_{zi_{FPA}} \cos(\Delta\alpha_u + \Delta a_{m_{z_{FPA}}} + \Delta\alpha_{BB}) \quad (15)$$

Equations (14) and (15) represent the accelerometer readings corrected to the wind axis system. The meaning of these values as they relate to the accelerometer force balance can be constructed by analyzing figure 3.

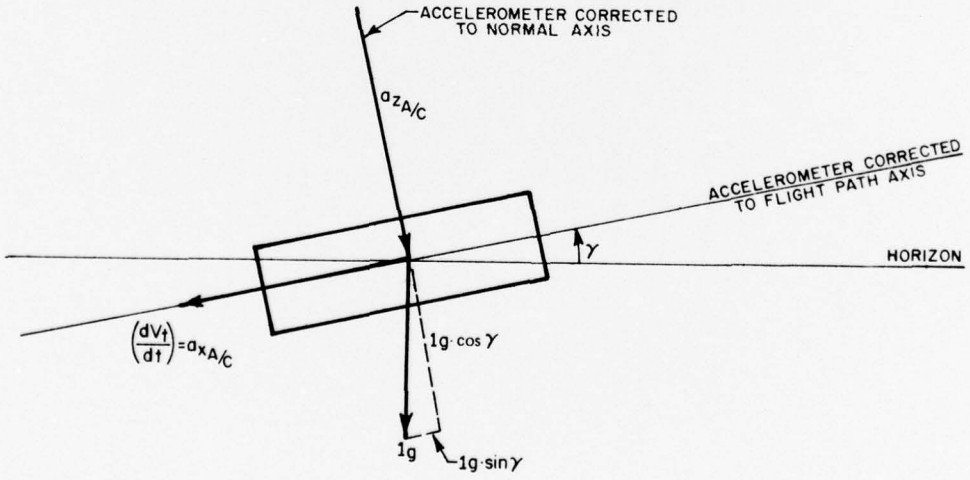

Figure 3
Transformed Axis Accelerometer Balance Diagram

13. Resolving the accelerations along and perpendicular to the flight path, the following equations are obtained:

$$a_{x_{FPA}} = a_{x_{A/C}} + g \sin\gamma \tag{16}$$

$$a_{z_{FPA}} = a_{z_{A/C}} + g \cos\gamma \tag{17}$$

or, again transforming the equations to load factor for convenience, the equations become:

$$n_{x_{FPA}} = \frac{a_{x_{A/C}}}{g} + \sin\gamma \tag{18}$$

$$n_{z_{FPA}} = \frac{a_{z_{A/C}}}{g} + \cos\gamma \tag{19}$$

By definition, the acceleration along the flight path of an aircraft ($a_{x_{A/C}}$) is the time rate of change of the true velocity along the flight path ($\frac{dV_t}{dt}$) which yields:

$$n_{x_{FPA}} = \frac{1}{g}\frac{dVt}{dt} + \sin\gamma \tag{20}$$

Combining equations (5) and (20):

$$F_{ex} \triangleq F_n - D = W\,(n_{x_{FPA}}) \tag{21}$$

Equation (21) is the singularly most important relation to the accelerometer method. It relates the wind axis longitudinal load factor with aircraft gross weight directly to excess thrust. Combining equations (9) and (19):

$$L = W\,(n_{z_{FPA}}) - F_g \sin(\alpha+\tau) \tag{22}$$

Equation (22) relates the wind axis normal load factor to aerodynamic lift.

14. In order to more fully develop the resolved accelerations as they fit into the picture of overall aircraft performance, the determination of longitudinal load factor can be further expanded with the aid of the velocity diagram of figure 4.

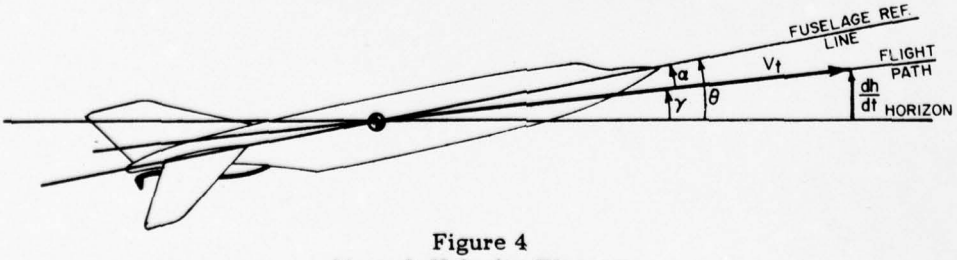

Figure 4
Aircraft Velocity Diagram

From the breakdown of the aircraft velocity components:

$$\sin\gamma = \frac{dh}{dt}\,\frac{1}{V_t} \tag{23}$$

combining equation (23) with equation (20):

$$n_{x_{FPA}} = \frac{1}{g}\,\frac{dVt}{dt} + \frac{dh}{dt}\,\frac{1}{V_t} \tag{24}$$

The specific energy (Es) of an aircraft is given by:

$$E_s = h + \frac{V_t^2}{2g} \tag{25}$$

and the time rate of change of specific energy is given by:

$$Ps = \dot{E}_s = \frac{dh}{dt} + \frac{V_t}{g}\,\frac{dV_t}{dt} = (n_{x_{FPA}})\,V_t \tag{26}$$

where equation (26) relates the time rate of change of specific energy and the longitudinal load factor at each velocity point.

15. It has been shown then, that the resolved components of longitudinal and normal load factor will yield information about the aircraft excess thrust and aerodynamic lift. Additionally, it has been shown that the longitudinal load factor together with velocity gives information with regard to the time rate of change of aircraft specific energy.

BODY MOUNTED ACCELEROMETER PACKAGE

16. The data analysis procedures for the body mounted package become more complex when it is considered that the body mounted accelerometer is not aligned with the flight path but stays near the fuselage reference line. Thus, angle of attack, as well as corrections to angle of attack, enter into the overall calculations. Therefore, errors in measured angle of attack will be introduced which were not present with the flight path accelerometer. The forces acting on the body accelerometer can be resolved by analyzing figure 5.

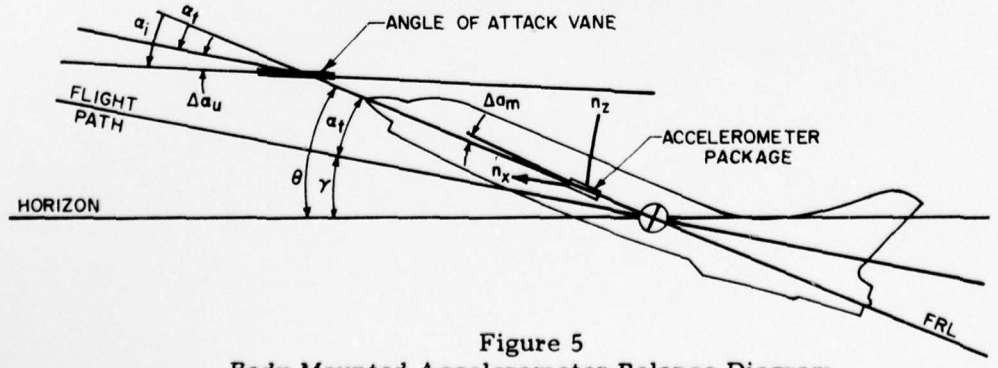

Figure 5
Body Mounted Accelerometer Balance Diagram

17. The angle of attack vane is misplaced by the upwash at the boom and any boom bending due to rate effects (further effects of angular rate are discussed in paragraphs 27 to 32) so that the true angle of attack is given by:

$$\alpha_t = \alpha_i + \Delta\alpha_{upwash} + \Delta\alpha_{BB} \tag{27}$$

The body accelerometer is further misplaced by a mechanical misalignment (Δa_m). Resolving accelerations parallel and perpendicular to the flight path (as with the flight path accelerometer), the following equations are obtained:

$$n_{x_B} = n_{x_{i_B}} \cos(\alpha_t + \Delta a_{m_{x_B}}) - n_{z_{i_B}} \sin(\alpha_t + \Delta a_{m_{z_B}}) \tag{28}$$

and $$n_{z_B} = n_{x_{i_B}} \sin(\alpha_t + \Delta a_{m_{x_B}}) + n_{z_{i_B}} \cos(\alpha_t + \Delta a_{m_{z_B}}) \tag{29}$$

and, with the use of figure 5, it can be seen that:

$$n_{x_B} = \frac{a_{x_{A/C}}}{g} + \sin\gamma \tag{30}$$

$$n_{z_B} = \frac{a_{z_{A/C}}}{g} + \cos\gamma \tag{31}$$

18. With the accelerometer readings referred to the wind axis system, figures 3 and 4 apply as well as the analysis of paragraphs 13, 14, and 15 so that equations (21), (22), and (26) apply as summarized below:

$$F_{ex} \triangleq F_n - D = W \cdot n_{x_B} \tag{32}$$

$$L = W(n_{z_B}) - F_g \sin(\alpha + \tau) \tag{33}$$

$$\dot{E}_s = (n_{x_B}) V_t \tag{34}$$

BANK ANGLE EFFECTS

AIRCRAFT FORCE BALANCE

19. In the general case, the aircraft will not maintain a wings level attitude so that it becomes necessary to evaluate the effect of bank angle on the equation set. Since the wind axis system is used, introducing bank angle into figure 1 induces a side force component in the weight vector equal in magnitude to W sin ϕ and the z direction component of weight becomes W cos γ cos ϕ. All other vectors remain the same since the axis system (for wind axis analysis) has rolled with the aircraft. Thus, equation (9) becomes:

$$L = W\left(\cos\gamma\cos\phi + \frac{a_{z_{A/C}}}{g}\right) - F_g \sin(\alpha + \tau) \tag{35}$$

FLIGHT PATH ACCELEROMETER

20. In the flight path accelerometer, the transformation equations under nonzero bank angle are unaffected since the accelerometer remains aligned with the wind axis system. The transformed accelerations of figure 3, however, show the effect of the 1 g vector being rotated out of plane so that equation (19) becomes:

$$n_{z_{FPA}} = \frac{a_{z_{A/C}}}{g} + \cos\gamma \cos\phi \tag{36}$$

when equation (36) is combined with equation (35), equation (22) is the result or:

$$L = W\left(n_{z_{FPA}}\right) - F_g \sin(\alpha + \tau) \tag{22}$$

In the wind axis system then, nonzero bank angle does not affect the equation set when the flight path accelerometer is used.

BODY ACCELEROMETER PACKAGE

21. In the body accelerometer, the problem is further complicated in that the accelerometer is not aligned with the flight path and must be transformed through the angle of attack. Resolving the accelerations along and perpendicular to the flight path, we obtain equation (29):

$$n_{z_B} = n_{x_{i_B}} \sin\left(\alpha_t + \Delta a_{m_{x_B}}\right) + n_{z_{i_B}} \cos\left(\alpha_t + \Delta a_{m_{z_B}}\right) \tag{29}$$

$$n_{z_B} = \frac{a_{z_{A/C}}}{g} + \cos\gamma \cos\phi \tag{37}$$

which again can be combined with equation (35) to yield:

$$L = W\left(n_{z_B}\right) - F_g \sin(\alpha_t + \tau) \tag{38}$$

It can be seen that the equation sets are unaltered by the addition of bank angle.

SIDESLIP EFFECTS

22. In the general case, small values of sideslip will cause a misalignment of the acceleration vectors in the lateral plane. As explained in reference (a), lateral misalignments (which are the equivalent of sideslip) create negligible errors if they are less than 3 degrees. If this assumption is too restrictive, the case of nonzero sideslip must be considered. Additionally, a three-axis accelerometer must be considered in that correcting the equations without lateral accelerations may be more in error than completely ignoring the correction. In the case of sideslip, the normal axis accelerations are not affected since they are perpendicular to the plane of action of sideslip. The corrective procedures for the flight path axis can be shown with figure 6.

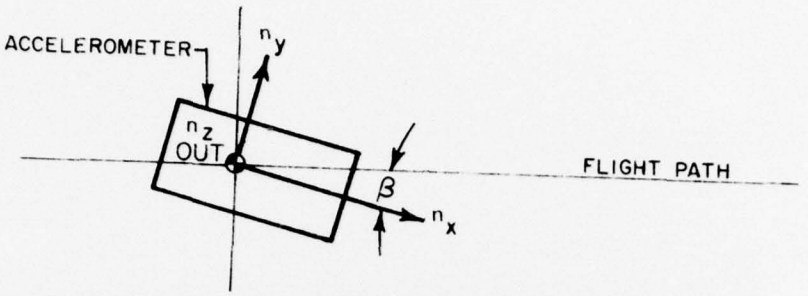

Figure 6
Accelerometer Sideslip Diagram

23. The n_x term is rotated out of plane by β, and a component of $n_y \sin \beta$ is introduced such that:

$$n_{x_{FP}} = n_x \cos \beta + n_y \sin \beta \tag{39}$$

The two terms tend to have a cancelling effect as shown in the diagram but this is not always the case.

FULLY DEVELOPED COORDINATE TRANSFORMATIONS

24. The fully developed equations for a three-axis system with bank angle and sideslip and no simplifying assumptions about misalignments are given below. Additionally, no angular rate or angular acceleration corrections are made. These will be dealt with in the next section. Finally, no cross-axis sensitivity has been introduced since it is basically a calibration problem and is dealt with in reference (a).

FLIGHT PATH ACCELEROMETER

25. The coordinate transformations for the flight path accelerometers are:

$$n_{x_{FPA}} = n_{x_i} \cos (\Delta\alpha_u + \Delta a_{m_{x_{FPA}}}) \cos \beta - n_{z_i} \sin (\Delta\alpha_u + \Delta a_{m_{x_{FPA}}}) \cos \beta + n_{y_i} \sin \beta \tag{40}$$

$$n_{z_{FPA}} = n_{x_i} \sin (\Delta\alpha_u + \Delta a_{m_{x_{FPA}}}) + n_{x_i} \cos (\Delta\alpha_u + \Delta a_{m_{z_{FPA}}}) \tag{41}$$

For additional detail discussion, consult reference (b).

BODY ACCELEROMETER

26. The coordinate transformations for the body mounted accelerometer package are:

$$n_{x_B} = n_{x_i} \cos(\alpha_t + \Delta a_{m_{x\beta}}) \cos\beta + n_{y_{i_B}} \sin\beta - n_{z_{i_B}} \sin(\alpha_t + \Delta a_{m_{z_B}}) \cos\beta \qquad (42)$$

and

$$n_{z_B} = n_{x_{i_B}} \sin(\alpha_t + \Delta a_{m_{x_B}}) + n_{z_{i_B}} \cos(\alpha_t + \Delta a_{m_{z_B}}) \qquad (43)$$

For additional detail discussion, consult reference (c).

ANGULAR RATE EFFECTS

27. The angular rate effect on an accelerometer located some distance from the cg induces accelerations which are reflected in the accelerometer readings.

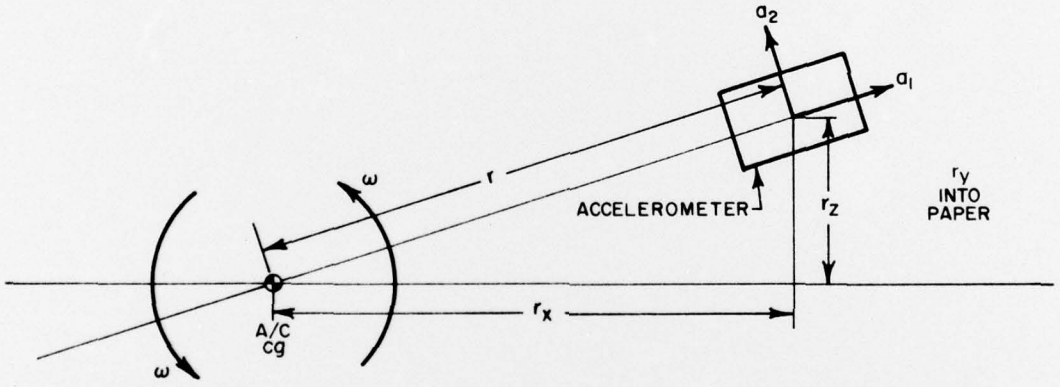

Figure 7
Rotational Dynamics

As illustrated in figure 7, the rotational rate (ω) creates an acceleration in the two axes of the plane of rotation. The centripetal acceleration (a_1) is created by the rotation as:

$$a_1 = r\omega^2 \qquad (44)$$

The rotational acceleration (a_2) is created by the rate of change of rotation rate as:

(45)

28. In the general case of rotation about all three axes, the cross product produces an acceleration perpendicular to the plane of rotation of a given pair of rotational vectors. In general, the accelerations as measured by the accelerometer can be corrected for angular rates and then corrected back to the cg. Alternately, the acceleration readings can be corrected to the cg and then the cg accelerations corrected for angular rates. For the body accelerometers, the latter method is easier and yields:

$$n_{x_{net}} = n_{x_i} + \frac{l}{g}\left[r_x(\dot{\theta}^2 + \dot{\psi}^2) + r_y(\ddot{\psi} - \dot{\phi}\dot{\theta}) + r_z(\ddot{\theta} + \dot{\phi}\dot{\psi})\right] \tag{46}$$

and

$$n_{z_{net}} = n_{z_i} + \frac{l}{g}\left[-r_x(\ddot{\theta} - \dot{\phi}\dot{\psi}) + r_y(\ddot{\phi} + \dot{\psi}\dot{\theta}) + r_z(\dot{\theta}^2 + \dot{\phi}^2)\right] \tag{47}$$

This method is employed in reference (b) which also includes corrective procedures for the lateral axis, i.e.:

$$n_{y_{net}} = n_{y_i} + \frac{l}{g}\left[-r_x(\ddot{\psi} - \dot{\phi}\dot{\theta}) + r_y(\dot{\phi}^2 + \dot{\psi}^2) - r_z(\ddot{\phi} - \dot{\psi}\dot{\theta})\right] \tag{48}$$

The corrected accelerations are computed by replacing $n_{x_{net}}$, $n_{z_{net}}$, and $n_{y_{net}}$ for n_{x_i}, n_{z_i}, and n_{y_i}, respectively, in the coordinate transformations. The corrected normal acceleration can then be used to compute boom normal acceleration to determine boom bending by:

$$n_{z_{BB}} = n_{z_B} + \frac{l}{g}\left[X\alpha(\ddot{\theta} + \dot{\phi}\dot{\psi}) - Y\alpha(\ddot{\phi} + \dot{\psi}\dot{\theta}) - Z\alpha(\dot{\theta}^2 + \dot{\phi}^2)\right] \tag{49}$$

Further effects of boom bending are discussed in reference (a).

29. For the flight path accelerometer, it becomes more convenient to correct the accelerations for angular rates at the accelerometer and then correct back to the cg. So that:

$$n_{z_{BB}} = n_{z_{FPA}} \tag{50}$$

and

$$n_{x_{FPA_{CG}}} = n_{z_{FPA}} + \frac{r}{g}\left[(\dot{\theta}^2 + \dot{\psi}^2)\cos\alpha - (\dot{\phi}\dot{\psi} - \ddot{\theta})\sin\alpha\right] \tag{51}$$

$$n_{z_{FPA_{CG}}} = n_{z_{FPA}} + \frac{r}{g}\left[(\dot{\theta}^2 + \dot{\psi}^2)\sin\alpha + (\dot{\psi}\dot{\phi} - \ddot{\theta})\cos\alpha\right] \tag{52}$$

where r is the distance from acceleromter to cg along a radial. This analysis technique together with a complete derivation of the above relation is presented in reference (b).

30. In summary, when dealing with body accelerometers, it is more convenient to correct the accelerometer readings to the cg prior to coordinate transformation. Thus, equations (46), (47), and (48) are employed prior to coordinate transformation, and equation (49) is used for boom bending calculations. When dealing with flight path accelerometers, it is more convenient to calculate the local acceleration at the accelerometers so that equation (50) can be used for boom bending calculations, and equations (51) and (52) are applied after coordinate transformation. Of course, either accelerometer package can mathematically be treated by either technique.

PRIMARY EQUATION SUMMARY

FLIGHT PATH ACCELEROMETER

31. The final accelerations along and perpendicular to the flight path are computed as:

$$n_{x_{FPA_{CG}}} = n_{x_i} \cos(\Delta\alpha + \Delta a_{m_{x_{FPA}}}) \cos\beta - n_{z_i} \sin(\Delta\alpha + \Delta a_{m_{z_{FPA}}}) \cos\beta + n_{y_i} \sin\beta + \frac{r}{g}\left[(\dot{\theta}^2 + \dot{\psi}^2) \cos\alpha_t - (\dot{\phi}\dot{\psi} - \ddot{\theta}) \sin\alpha_t\right] \quad (53)$$

and

$$n_{z_{FPA_{CG}}} = n_{x_i} \sin(\Delta\alpha + \Delta a_{m_{x_{FPA}}}) + n_{z_i} \cos(\Delta\alpha + \Delta a_{m_{z_{FPA}}}) + \frac{r}{g}\left[(\dot{\theta}^2 + \dot{\psi}^2) \sin\alpha_t + (\dot{\psi}\dot{\phi} - \ddot{\theta}) \cos\alpha_t\right] \quad (54)$$

where $\Delta\alpha = \sum_{i=1}^{n} \Delta\alpha_i$ or $\Delta\alpha$ is the total of all corrections to angle of attack as detailed in reference (d).

BODY MOUNTED ACCELEROMETER

32. The final accelerations along and perpendicular to the flight path are computed as:

$$n_{x_{B_{CG}}} = n_{x_{net}} \cos(\alpha_t + \epsilon_{x_B}) \cos\beta - n_{z_{net}} \sin(\alpha_t + \epsilon_{z_B}) \cos\beta + n_{y_{net}} \sin\beta \quad (55)$$

and

$$n_{z_{B_{CG}}} = n_{x_{net}} \sin(\alpha_t + \epsilon_{x_B}) + n_{z_{net}} \cos(\alpha_t + \epsilon_{z_B}) \tag{56}$$

where

$$n_{x_{net}} = n_{x_{i_B}} + \frac{1}{g}\left[r_x(\dot{\theta}^2 + \dot{\psi}^2) + r_y(\ddot{\psi} - \dot{\phi}\dot{\theta}) + r_z(\ddot{\theta} + \dot{\phi}\dot{\psi})\right] \tag{57}$$

$$n_{z_{net}} = n_{z_{i_B}} + \frac{1}{g}\left[-r_x(\ddot{\theta} - \dot{\phi}\dot{\psi}) + r_y(\ddot{\phi} + \dot{\psi}\dot{\theta}) + r_z(\dot{\theta}^2 + \dot{\phi}^2)\right] \tag{58}$$

and

$$n_{y_{net}} = n_{y_{i_B}} + \frac{1}{g}\left[-r_x(\ddot{\psi} + \dot{\phi}\dot{\theta}) + r_y(\phi^2 + \psi^2) - r_z(\ddot{\phi} - \dot{\psi}\dot{\theta})\right] \tag{59}$$

AIRCRAFT FORCE BALANCE

33. With the measured quantities corrected and resolved to the proper axes, the primary equations for the determination of aircraft excess thrust, lift, and time rate of change of specific energy are as follows:

$$F_{ex} \triangleq F_n - D = W \cdot n_x \tag{60}$$

$$L = W \cdot n_z - F_g \sin(\alpha_t + \tau) \tag{61}$$

$$\dot{E}_s = n_x V_t \tag{62}$$

where

$$n_x = n_{z_{B_{CG}}} \text{ or } = n_{x_{FPA_{CG}}} \tag{63}$$

and

$$n_z = n_{z_{B_{CG}}} \text{ or } = n_{z_{FPA_{CG}}} \tag{64}$$

The latter equations depend only on the accelerometer package in use.

34. The aircraft force balance equations can now be expanded to yield the normal aircraft performance parameters as follows:

Equation (60) becomes:

$$C_D = \frac{F_n - W \cdot n_x}{q \quad s} = \frac{F_n - W \cdot n_x}{1/2 \rho \, V_t^2 S}$$

$$= \frac{F_n - W \cdot n_x}{\frac{\gamma_a}{2} P_a M^2 S} \qquad (65)$$

Equation (61) becomes:

$$C_L = \frac{W \cdot n_z - F_g \sin(\alpha_t + \tau)}{1/2 \rho \, V_t^2 S}$$

$$= \frac{W \cdot n_z - F_g \sin(\alpha_t + \tau)}{\frac{\gamma_a}{2} P_a M^2 S} \qquad (66)$$

35. Equations (60) through (62) are convenient when applying flight test data to the direct methods of determining aircraft performance, while equations (65) and (66) are more convenient when applying flight test data to the indirect methods of determining aircraft performance.

CONCLUDING REMARKS

36. The aircraft accelerations yield very useful data for defining aircraft performance. Extreme care, however, must be exercised when using measured accelerations to insure proper values of resolved accelerations. These resolved acceleration values are directly adaptable to either the direct or indirect methods of determining aircraft performance.

REFERENCES

(a) Simpson, W. R., Developing the Airplane Drag Polar and Lift Slope Curve from Flight Test Data Using On-Board Accelerometers, Flight Test Technical Memorandum No. 5-73, U.S. Naval Air Test Center, Patuxent River, Maryland, of 15 May 1973.

(b) Dunlap, E. W., and Porter, M. B., Theory of the Measurement and Standardization of In-Flight Performance of Aircraft, USAF Document No. F7C-TD-71-1, Edwards Air Force Base, Edwards, California, of Apr 1971.

(c) Pueschel, P., Development of Dynamic Methods of Performance Flight Testing, Report No. ADR-07-01-70.1, Grumman Aerospace Corporation, Bethpage, New York, Aug 1970.

(d) Simpson, W. R., The Determination of Aircraft Angle of Attack, Flight Test Technical Memorandum No. 2-75, U.S. Naval Air Test Center, Patuxent River, Maryland, of 27 Mar 1975.

(e) USAF Aerospace Research Pilot School, Performance, USAF Document No. FTC-T1H-70-1001, Edwards AFB, Edwards, California, of May 1970.

LIST OF SYMBOLS

Symbol	Definition	Common Units	Metric Units
a_1, a_2	Acceleration in the subscripted direction	ft/sec^2	(m/sec^2)
a	Accelerometer	-	-
C_{L_α}	Lift coefficient partial derivative with angle of attack	1/radians	(1/radians)
cg	Center of gravity	% MAC	(% MAC)
D	Drag force	lb	(N)
d	Derivative indicator (differential)	-	-
E_s	Specific Energy	ft	(m)
F	Force, thrust, drag, etc., with subscript	lb	(N)
g	Acceleration of gravity	ft/sec^2	(m/sec^2)
h	Altitude	ft	(m)
L	Lift	lb	(N)
ℓ	Length	ft	(m)
M	Mach number	None	None
m	Mass	Slug	(kg)
MAC	Length of the mean aerodynamic chord	ft	(m)
n	Load factor in the subscripted direction	None	None
P_a	Ambient pressure	lb/ft^2	(N/m^2)
q	Dynamic pressure	lb/ft^2	(N/m^2)
r	Radius or distance in subscripted direction	ft	(m)

Symbol	Definition	Common Units	Metric Units
S	Area of wing	ft^2	(m^2)
t	Time	sec	-
V	Velocity (airspeed)	ft/sec	(m/sec)
W	Weight	lb	(N)
W_a	Airflow	slugs/sec	(kg/sec)
Greek Symbols			
α	Angle of attack (aircraft reference above flight path positive)	deg	(deg)
β	Sideslip angle	deg	(deg)
γ	Flight path angle (climb attitude positive)	deg	(deg)
Δ	Change or correction to a parameter	-	-
Δ_{a_m}	Misalignment (with subscripts)	deg	(deg)
ζ	Damping ratio	None	None
θ	Pitch attitude (nose up positive)	deg	(deg)
$\Delta\alpha_{BB}$	Boom bending	deg	(deg)
π	3.14159	None	None
σ	Aircraft heading	deg	(deg)
Σ	Summation	-	-
τ	Thrust inclination angle (longitudinal offset)	deg	(deg)
ρ	Air density	$slugs/ft^3$	(kg/m^3)

Symbol	Definition	Common Units	Metric Units
$\emptyset$	Bank angle (right wing down positive)	deg	(deg)
ψ	Yaw angle (airplane nose right positive)	deg	(deg)
ω	Angular rate	deg/sec	(deg/sec)
ω_n	Natural frequency	cycles/sec	(cycles/sec)
ω_d	Damped frequency	cycles/sec	(cycles/sec)
γ_a	Ratio specific heats for air - 1.40 at Standard temperature	-	-

Subscripts and Superscripts

( ) A/C	Aircraft
( ) B	Body reference
( ) BB	Boom bending
( ) ex	Excess
( ) FPA	Flight Path Accelerometer
( ) g	Gross
( ) i	Indicated
( ) m	Misalignment
( ) n	Net
( ) o	Initial condition
( ) p	Pitch rate
( ) r	Ram
( ) T, t	True quantity
( ) u, upwash	Upwash
( ) x	X-axis (flight path)
( ) y	Y-axis (lateral)

Symbol	Definition	Common Units	Metric Units
( ) z	Z-axis (flight path perpendicular)		
( ) 1, 2, 3, 4	Condition point		
$(\dot{})$	First time derivative		
$(\ddot{})$	Second time derivative		
$\triangleq$	Equal by definition		

DISTRIBUTION:

AFFDL (ASD)	(2)
AFFTC	(2)
NAVAIR (AIR-530)	(2)
ARPS	(2)
NASA, FRC	(2)
NASA, Langley	(2)
AFFSD	(2)
DDC	(2)
USNTPS	(2)
NAVAIRTESTCEN (SA-43)	(10)
NAVAIRTESTCEN (SA)	(2)
NAVAIRTESTCEN (SY)	(2)
NAVAIRTESTCEN (AT)	(2)